CIMAC CONGRESS 25
ZURICH, MAY 19 – 23, 2025

2025 | 114

Towards conceptual understanding of pre-ignition mechanisms in hydrogen-fueled engines

Basic research & advanced engineering - new concepts

Ales Srna, Sandia National Laboratories

Taesong Lee, Sandia National Laboratories
Vasco Duke, Sandia National Laboratories
Rajavasanth Rajasegar, Colorado School of Mines

ABSTRACT

Pre-ignition is a key barrier to reaching diesel-like power density, low-end torque and efficiency in hydrogen engines. The complexity of underlying processes and range of potential pre-ignition sources (hot-spots, combustion residuals, glowing particles, carbonaceous deposits and oil droplets) make efficient mitigation of this abnormal combustion phenomenon a challenging endeavour, further aggravated by the lacking conceptual understanding of underlying mechanisms. To this end, Sandia has developed an extensive framework to study pre-ignition using “controlled” artificial pre-ignition sources in a heavy-duty hydrogen optical engine to develop a conceptual understanding of the underlying mechanisms behind individual sources and to propose effective mitigation strategies. This lecture will cover the recent progress on this path – covering the aspects of hot-spot pre-ignition, the role of catalytically-active surfaces, the effects of hydrogen on auto-ignition of oil-vapors and the influence of hot combustion residuals. We will explain the mechanisms of hot-spot pre-ignition suppression through delayed hydrogen injection, show that catalytic surfaces play a minimal role in pre-ignition, explore the role of combustion residuals on pre-ignition, and outline the interplay between oil droplet size, evaporation and chemical interactions between hydrogen and oil that jointly govern the oil-induced pre-ignition.

1 INTRODUCTION:

The recent regulatory trends in Europe, United States (US) and elsewhere impose formal or informal (through fleet CO_2 emission limits) light-duty and heavy-duty sales mandates for vehicles assumed to produce “zero-emissions” (ZEV). Some legislative bodies (California Air Resource Board, for example) impose rigid ZEV definitions based on presence of a tailpipe (zero pollutant and green-house gas tailpipe emissions under all operating conditions) with arguably negative implications for fast decarbonisation of transportation [1]. Similarly, many of the US incentives for low-carbon transportation technologies rely on an equally rigid ZEV definition. However, a more pragmatic approach is currently proposed in the European Union and by the US Environment Protection Agency (EPA). Under these proposed rules, hydrogen-fueled internal combustion engine (H2ICE) powered vehicles will receive a full ZEV credit. This development sparked a considerable interest in developing H_2-fueled powertrains, with H2ICE benefiting from lower upfront cost, established supply-chain and customer/service familiarity/acceptance relative to fuel-cell powertrains. Numerous engine OEMs announced their plans for near-term (1-5 years) market introduction of H2ICE. In addition, the H2ICE have the additional benefit of lower engine-out nitrogen oxides (NOx) emission relative to traditional diesel engine powertrains and exhaust temperature range that is well-suited for efficient de-NOx after-treatment. As a fuel, hydrogen (H_2) has several properties that make it attractive for combustion applications, such as wide flammability limits, high flame speed [2, 3], good auto-ignition resistance [4], and the fact that it can be produced using renewable energy sources [5]. Nevertheless, challenges associated with reduced efficiency, lower power density, and costly, bulky on-board fuel storage relative to diesel engine counterparts are the main barriers to fast market introduction and penetration of H2ICE.

The low volumetric density of H_2 aggravates the power density challenge of H2ICE, however, adoption of direct fuel injection can somewhat alleviate this limitation [6]. The other, more significant, challenge to H2ICE power density and efficiency is abnormal combustion, which includes pre-ignition and knock. The high auto-ignition resistance of H_2 under engine conditions can help to avoid knock, however, the low H_2 minimum ignition energy makes H_2 especially prone to pre-ignition [7, 8]. Here, pre-ignition is defined as the spontaneous initiation of combustion ahead of the desired ignition timing, and results in high in-cylinder pressure and/or combustion knock [9, 10]. If pre-ignition occurs during the intake stroke, the flame can also propagate into the intake port and may compromise its mechanical integrity – a particularly high risk for port-injected designs.

The pre-ignition mitigation approaches suggested in the literature include reduction of crevice volumes in engines (top-land, valve crevice, spark-plug insulator gap) [11-13], avoidance of noble-metal spark electrodes [14], cool spark-plug ratings, ignition systems which avoid ghost sparks, special ring-pack design and adoption of ultra-clean combustion chambers. All of these approaches contribute to mitigation of pre-ignition and the default hardware choices for H2ICE likely already include these modifications. Nevertheless, these modifications are usually insufficient to achieve incumbent diesel engine power density or to allow high compression-ratio engine operation to approach diesel-like engine efficiency [15]. Typically, the H2ICEs adopt compression ratios lower than in contemporary natural gas engines and operate at very lean air-to-fuel ratios to fully mitigate pre-ignition. The low compression ratio negatively affects efficiency while the requirement for ultra-lean combustion limits power density and transient response. These challenges elucidate the need for understanding of the underlying pre-ignition mechanisms and phenomenology to enable more effective mitigation strategies.

Despite the wealth of knowledge on low-speed pre-ignition in gasoline direct-injection (GDI) engines, H_2 fuel does not wet cylinder walls, which is a key cause of pre-ignition in GDI engines [16]. Though turbulent mixing with colder boundary layers prolongs ignition delay, pre-ignitions especially at lower pressures and increased ignition delay times have been attributed to the thermal diffusivity of the mixture [17], which becomes significant in the case of H_2. Several potential mechanisms of pre-ignition identified in the literature are illustrated in Figure 1. These include hot-spots in combustion chamber (exhaust valves, spark plug) [11-13], catalytic effects of the platinum spark-electrodes [14], hot residuals from previous cycle [18], auto-igniting oil-droplets, hot particles, hot (carbonaceous) deposits on engine walls [19] and slowly-burning flames in the top-land crevice [20]. The plethora of potential sources of pre-ignition, lack of the fundamental understanding behind each individual mechanism, and a wide range of engine designs in the market makes efficient mitigation of pre-ignition challenging. With the lack of systematic studies of pre-ignition under controlled conditions, it is often unclear which pre-ignition mechanism is dominant. In port-injected engines, optimization of valve and injection timing can often reduce the back-fire tendency by reducing the interaction of fresh charge with hot exhaust residuals [11, 21]. At higher loads and with direct-injection technologies, other pre-ignition mechanisms become dominant.

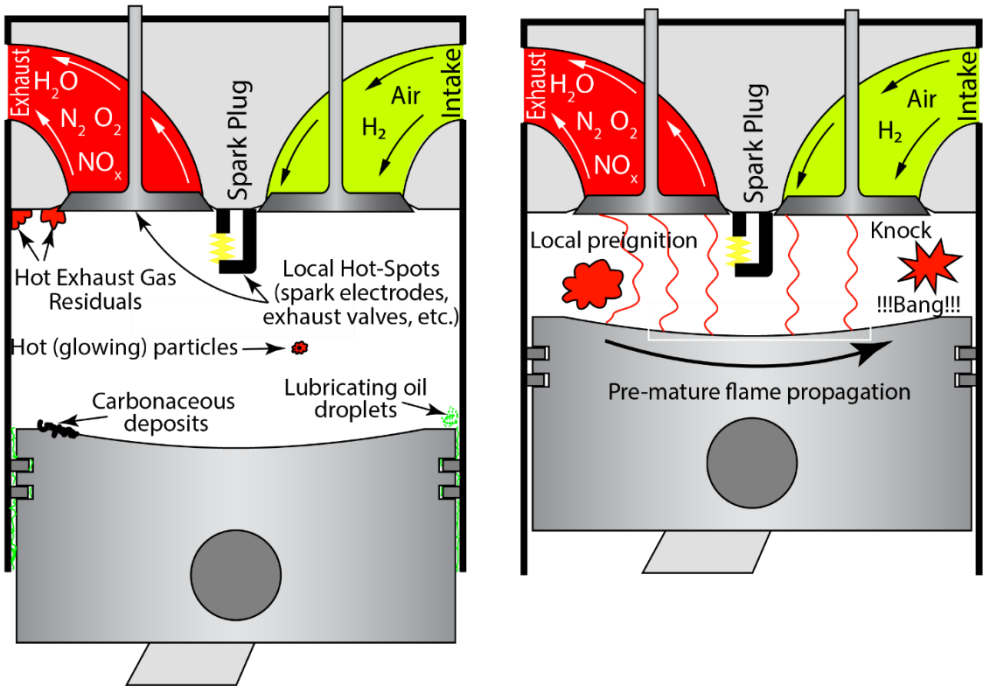

Figure 1: Conceptual schematic of pre-ignition mechanisms inside the engine combustion chamber (left) and an illustration of pre-ignition and coupled knock phenomenology (right).

This work offers an overview of experimental activities conducted at Combustion Research Facility, Sandia National Laboratories, to gain insights and conceptual understanding of the underlying mechanisms governing pre-ignition in H2ICEs. For this purpose, a concept of "induced pre-ignition" was applied in a heavy-duty optical engine i.e., artificial controllable ignition sources were introduced into the engine combustion chamber, while optical diagnostics are used to visualize the pre-ignition timing, evolution and phenomenology. The paper first introduces the experimental methodology and optical diagnostics, followed by an overview of experimental results and conclusions for each of the tested pre-ignition mechanisms. Future plans are outlined at the end, followed by brief conclusions.

2 EXPERIMENTAL SETUP AND CONDITIONS

The experiments were conducted in Sandia Heavy-Duty Optical Engine laboratory, which features a Bowditch-design heavy-duty optical engine with displacement of 2.34 L derived from a single-cylinder version of the Cummins N14 diesel engine. This engine features a low-swirl flat cylinder head and a quiescent combustion chamber design with a cylindrical bowl and flat piston window. One of the two exhaust valves in this engine was replaced with a window to enable visualization of combustion phenomena near the cylinder liner wall in addition to visualization through piston and liner windows.

The laboratory is equipped with a H_2 fueling system that can supply fumigation/port injection and/or medium-pressure direct injection. For safety reasons, flame arrestors are mounted in the intake and exhaust runners about ~20 cm from the cylinder head, which impacts intake and exhaust pressure dynamics as explained in section "Residual-induced pre-ignition". Details about the optical engine and fueling system are listed in Table 1.

Table 1. Sandia Heavy-Duty Optical Engine specifications

Engine Specifications	
Base engine	Cummins N-14, diesel
Number of cylinders	1
Combustion chamber	Quiescent, direct injection
Swirl ratio	0.5
Bore x Stroke [mm]	139.7 x 152.4
Compression ratio	10.3:1 or 11.2:1 (config. dependent)
Piston bowl properties	Cylindrical bowl, 97.8mm wide, 15.5mm deep
Displacement [liters]	2.34

Table 2. Fueling system and auxiliary combustion chamber components specifications

Direct H2 injector	
Model	PHINIA, DI-CHG10 Outward-opening
Flow rate	Up to 10 g/s of H2, at 40 bar rail pressure
Mounting location	Centrally mounted; or side-mount in cylinder liner
Diesel injector	
Model	Delphi DFI 1.5, solenoid actuated
Nozzle arrangement	8x 131 µm, 156° included angle
Fuel	*n*-heptane
Glow plug characteristics	
Type	Bosch Duraspeed
Mounting location	16 mm below firedeck 13 mm radially inwards from cylinder wall
Maximum temperature	1570 K (nominal) 1210 K (tested during engine operation)

The flexibility of our optical engine allows us to rapidly change the injection and optical diagnostics configuration to investigate the targeted combustion processes or to simulate pre-ignition mechanisms like in the present work. Figure 2 outlines key components of the optical engine and illustrates three different setups used in present work to study a) pre-ignition by hot combustion residuals, b) hot-spot pre-ignition [22], and c) oil-induced pre-ignition [23].

The investigations of residual-driven pre-ignition (Figure 2a) were conducted with the engine operated in fumigation-injection mode using a scavenged pre-chamber system for reliable ignition. The spark timing and mixture equivalence ratio were varied to control the temperature and oxygen content of the combustion residuals that the fresh air/fuel mixture mixes with as it enters the combustion chamber. Fumigation fueling was selected as the worst-case scenario for pre-ignition and back-fire. This strategy creates a premixed fuel-air mixture by injecting hydrogen into the intake runner about 0.7 m upstream of the flame arrestor and the intake manifold. Thus the fresh mixture introduced into the combustion chamber at intake valve opening (IVO) readily contains fuel. The less pre-ignition prone PFI strategies introduce fuel during the middle of the intake stroke, so that the combustion residuals are first cooled by mixing with fresh air before fuel is introduced. The fueled pre-chamber as an igniter serves two purposes: it provides reliable ignition and fast combustion even when sparking late during the expansion stroke, and it traps combustion residuals, which undergo mixing with fresh mixture later in the cycle relative to residuals in the main chamber. Therefore, we can simultaneously study pre-ignition by two types of residuals and evaluate their pre-ignition propensity. The engine is skip-fired with one ignited cycle in every sequence of 20 cycles to protect the optical windows and exhaust valve from heat damage. Fumigation fueling was active for 6 cycles preceding the fired cycle to ensure that the targeted fuel-air equivalence ratio is achieved and maintained during the fired and the subsequent cycle while minimizing fuel consumption and the flammability of mixture in the exhaust surge tank [24]. High-speed OH* chemiluminescence (flame tracking) and IR (infrared) emission of hot water vapor (residuals) were collected throughout the intake and compression stroke of the cycle after the fired cycle to visualize any potential pre-ignition event. OH* and IR images were recorded with 1°CA and 2°CA resolution, respectively.

The experimental arrangements for the investigation of hot-spot pre-ignition and the preliminary investigations into oil-induced pre-ignition are only briefly summarized below since they were described in detail in our past publications [22, 23]. To investigate hot-spot pre-ignition (Figure 2b), an artificial, controllable, electrically heated hot-spot was mounted in the cylinder-liner window insert 16 mm below the firedeck, protruding 13 mm from the liner into the engine combustion chamber. The temperature of the hot-spot was calibrated using a thin-wire thermocouple and monitored during the engine operation using IR imaging. Two types of hot-spot were tested – a conventional ceramic hot-spot and a platinum-coated hot-spot featuring a 500 nm Pt coating over the ceramic to investigate the role of catalytic effects on pre-ignition propensity relative to a non-catalytic surface. Direct injection with varied injection timing was used to control the time when the fuel first interacts with the hot spot. High-speed OH* imaging at a 10 kHz frame rate was used to visualize the pre-ignition process and pin-point the timing of pre-ignition.

Finally, Figure 2c shows the setup used for preliminary investigations of oil-droplet induced pre-ignition. A diesel injector was used to inject n-heptane into a well-mixed mixture of H_2 and air with varying equivalence ratios under otherwise unchanged conditions. These tests highlight the impact of H_2 on the auto-ignition process of vaporized hydrocarbons (using n-heptane as surrogate), assuming that auto-ignition is the main driver of oil-induced pre-ignition. Two intensified high-speed cameras recorded the chemiluminescence of cool-flame and OH* as markers of first-stage and high-temperature ignition, respectively. The temporal resolution was

0.25°CA. This is only the first step in a comprehensive plan to unravel different aspects of oil-induced pre-ignition that includes oil droplet evaporation and coking testing as described in the future work section.

3 RESULTS AND DISCUSSION

3.1 Hot-spot pre-ignition and surface catalytic effects

Hotspot pre-ignition sequence is shown in Figure 3, as observed through the cylinder head window above the glow plug, with the glow-plug positioned in the top-left corner of the image. As H_2 autoignites near the hot surface, the first weak OH* emission is visible on the second image panel. The flame kernel grows and initially spreads away from the glow plug, followed by a flame propagation along the glow-plug stem towards the cylinder wall. Flame recordings, as shown in Figure 3, were used to determine whether pre-ignition has occurred and to pinpoint its timing

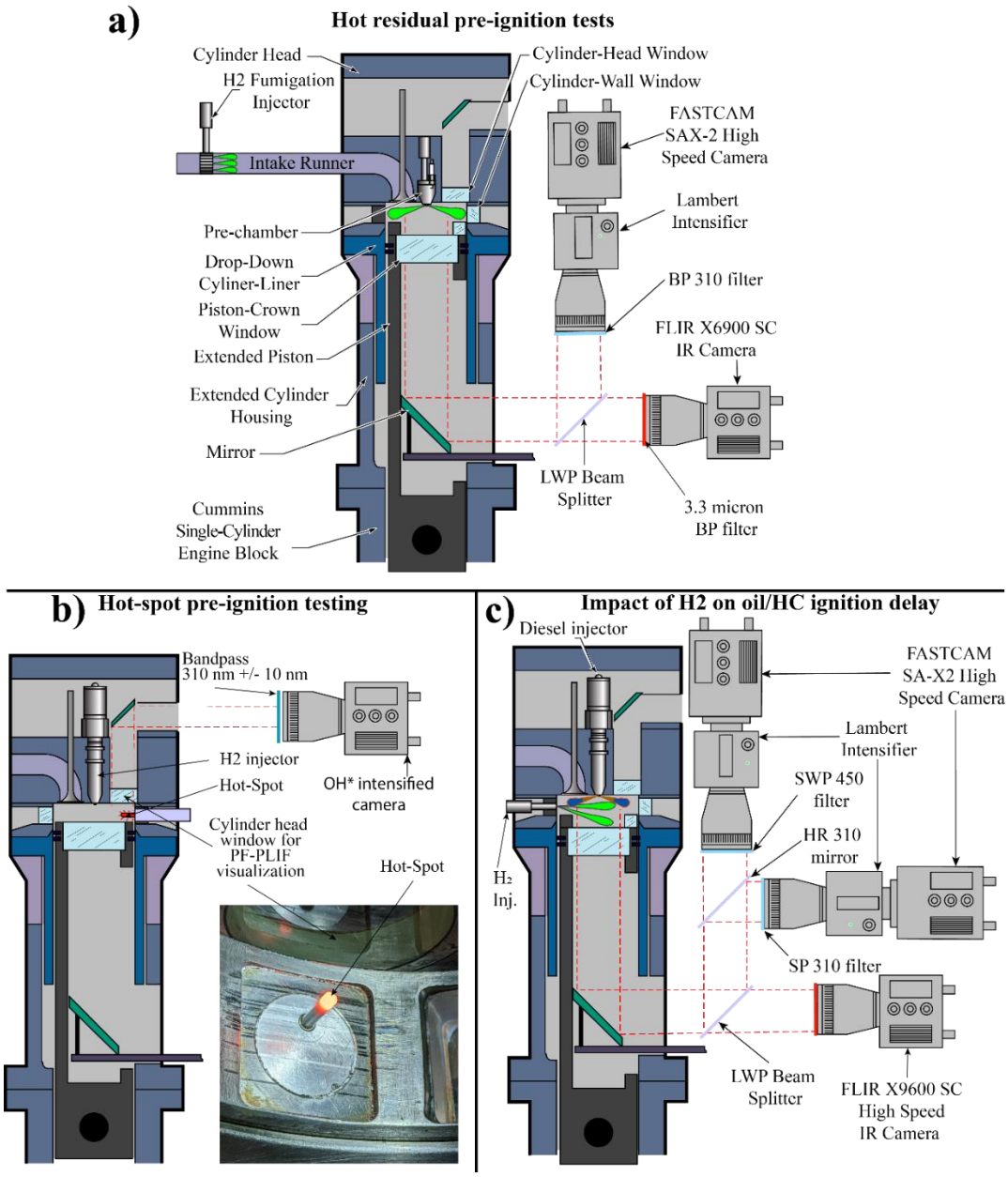

Figure 2: a) Schematic of the imaging system and the optical engine equipped with a pre-chamber for testing the role of combustion residuals on pre-ignition, with labeled major components. b) Glow-plug and imaging system arrangement for exploring the hot-spot pre-ignition. c) Injector and imaging system arrangement for exploring the impact of H2 on oil vapor ignition

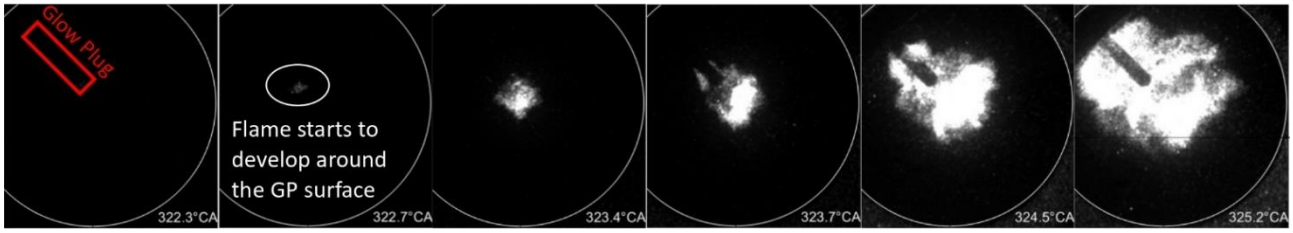

Figure 3: OH* chemiluminescence visualization of a hot-spot pre-ignition cycle.

The results of the above analysis are summarized in Figure 4 for early injection during the intake stroke (SOI = 20 CA) and a later injection during the compression stroke (SOI = 240 CA). Each panel presents the calculated timing of pre-ignition onset for a test run consisting of 50 cycles with fuel injection. Cycles that do not pre-ignite are grouped at the top of each panel and labeled accordingly. The corresponding cylinder pressure for each crank-angle on the left ordinate axis are shown for reference using the secondary axis. For each injection timing, the temperature of the hot spot was progressively increased (in steps of 0.1 V on the supply voltage corresponding to about ~12 K temperature change) so as to initiate a gradual transition from test runs with almost no cycles undergoing pre-ignition to a majority of cycles (> 70%) pre-igniting. This glow-plug temperature sweep is indicated by different colored markers shown in Figure 4.

For the earliest injection timing presented in Figure 4, i.e., SOI = 20°CA, it can be seen that for a hot-spot temperature of 1047 K, around ~55% of the cycles pre-ignite, with around 15% of these cycles igniting during the intake stroke (before 150°CA). This phenomenon, commonly referred to as backfire or flashback [14, 21], is characterized by the occurrence of pressure waves travelling inside the intake port as combustion tends to “flashback” into the intake system. This issue represents a major hurdle to overcome in the development of H2ICE due to the high flammability of the fuel, which is further exacerbated in port-fuel injection systems due to the presence of combustible mixture in the intake port.

As the glow-plug temperature is further increased to 1062 K, around ~85% of the cycles tend to pre-ignite with nearly half of them resulting in backfire. Finally, at a temperature of 1077 K, almost all of the cycles pre-ignited during the intake stroke. This temperature sweep indicates a high sensitivity of the pre-ignition phenomenon to the hot-spot temperature, given that a variation of only 12 K was sufficient to cause pre-ignition in a majority of the engine cycles. Regardless of the glow-plug temperature, the pre-ignition timings are clustered during the intake or early compression stroke, with no pre-ignitions occurring towards the TDC when in-cylinder pressure and temperature are highest. This counter-intuitive finding will be explored later in this section.

Similar sweeps were performed with later injection timings of 180 CA, 240 CA, 270 CA and 300 CA – for brevity, only the results for injection at the most interesting injection timing of 240 CA are presented (Figure 4b). For ceramic glow-plug temperatures below 1100 K, only one single cycle out of the 50 cycles pre-ignited. As discussed earlier, the sensitivity of pre-ignition to the hot-spot temperature is again evident here: At a glow-plug temperature of 1122 K, about 40% of the cycles pre-ignite with nearly all cycles undergoing pre-ignition for temperatures exceeding 1137 K. However, in stark contrast to the early injection timing cases discussed previously, the timing of pre-ignition onset displays a much smaller spread of nominally around ~10-30°CA centered at around ~300°CA, i.e., the onset of pre-ignition appears to be less stochastic with glow-plug temperatures seemingly not affecting this trend. This indicates a more repeatable flow and formation of mixture near the glow-plug when the injection timing is delayed from the BDC.

.

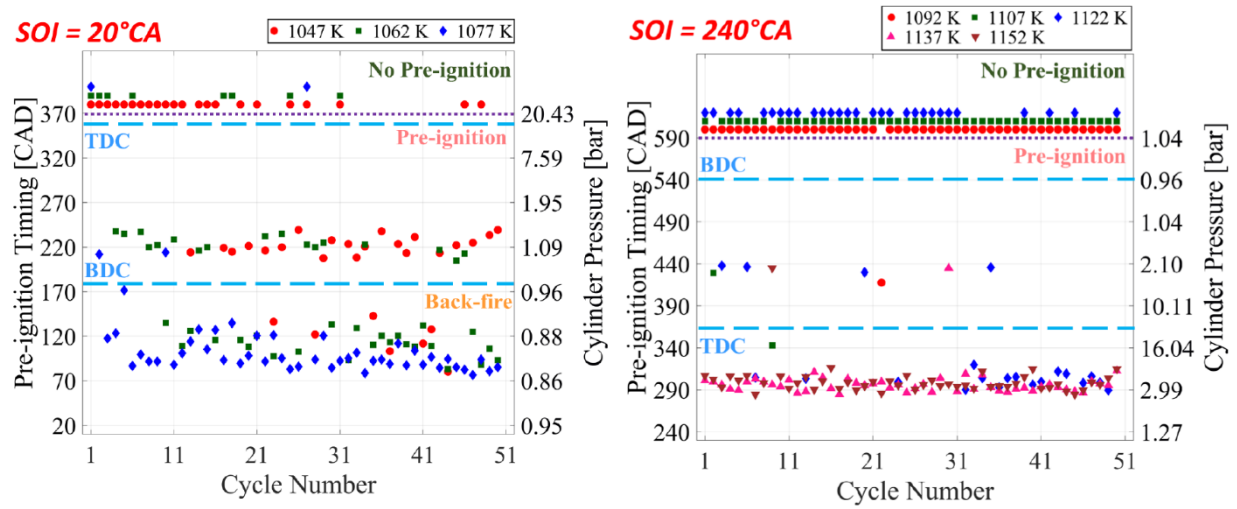

(a) SOI = 20°CA (b) SOI = 240°CA

Figure 4: Pre-ignition timing and probability depending on the injection timing, hot-spot temperature for a stock ceramic glow-plug.

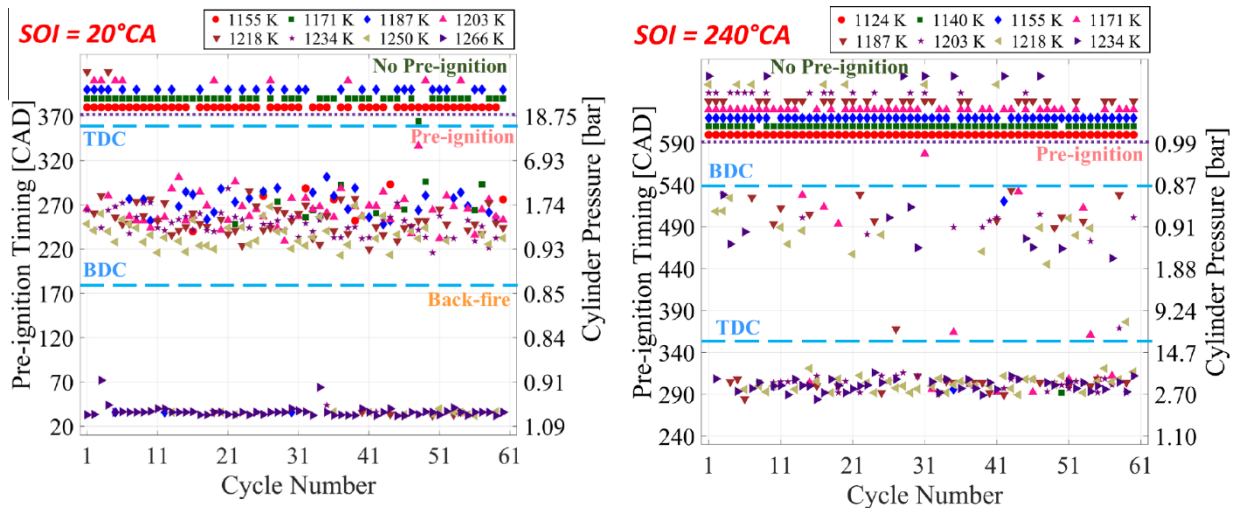

(a) SOI = 20°CA (b) SOI = 240°CA

Figure 5: Pre-ignition timing and probability depending on the injection timing, hot-spot temperature for a Platinum-coated glow-plug.

The behavior of the platinum (Pt) coated glow-plug (Figure 5a) pre-ignition indicates that a higher surface temperature (~100 K) is required to produce pre-ignition with a similar frequency relative to the baseline ceramic glow-plug (Figure 4a). At temperatures that created significant pre-ignition with a ceramic glow-plug, the Pt-coated glow-plug did not cause any pre-ignition. Another notable difference is a reduced tendency to back-fire, with most pre-ignition timings scattered during the early compression stroke. Only the highest tested temperature produced back-fire, which occurred almost immediately after the SOI, likely as soon as H_2 contacted the hot surface. This suggests that the surface catalytic activity is not a key factor in triggering hot-spot pre-ignition, with residence time of gases near the hot-spot playing a more significant role. Surface roughness might be relevant as well, though no further evidence can be provided here.

When the injection was delayed into the compression stroke (Figure 5b, SOI = 240°CA), the Pt-coated glow-plug showed similar behaviour to the ceramic glow plug (Figure 4b). However, Pt coated glow-plug required a higher temperature (~30 K) to trigger pre-ignition compared to stock ceramic glow-plug. The difference in pre-ignition timing between ceramic and Pt-coated hot-spots observed with earlier injection timing is no longer observable at later injection timings, aside from a higher tendency to trigger ignition late in the expansion stroke (after 360 CA) which technically does not constitute a pre-ignition. The

investigations also demonstrated that certain engine operating conditions temporarily and reversibly change the surface properties of Pt coating that increases the catalytic activity and the reactivity. This well-repeatable phenomenon is subject to further investigations in collaboration with catalysis experts.

To explain the sensitivity of H_2 ignition delay to pressure, temperature and equivalence ratio, constant-pressure homogeneous reactor calculations were conducted. The results provide further insight into the mechanisms governing the pre-ignition behavior presented in Figures 4 and 5. Each data-point on Figure 6 presents a false-color coded ignition delay result from an individual reactor simulation at a set initial pressure and temperature using the kinetic mechanism from [25]. The ignition delay quickly decreases with increasing temperature as expected. A significant sensitivity of ignition delay to pressure is observed, with ignition delay sharply increasing until a critical pressure is reached, indicating deactivation of the fast low-pressure reaction pathway. This critical pressure increases with temperature and exhibits a mild sensitivity to equivalence ratio – the critical pressure is somewhat decreased at higher equivalence ratio. The observed pressure sensitivity is opposite of trends typical for hydrocarbon fuels for which increasing pressure reduces the ignition delay. This trend also explains the low probability of hot-spot pre-ignition occurring at high pressure near the TDC, despite the high charge temperature. The lower probability of hot-spot pre-ignition at high pressure opens a potential pre-ignition mitigation strategy of injecting fuel later during the compression stroke when in-cylinder pressure readily exceeded the critical pressure required to ensure a longer ignition delay. The required condition for this strategy is that sufficiently fast mixing can be achieved. Other pre-ignition mechanisms might have different sensitivity to pressure and temperature and will be explored in the next sections.

3.2 Impact of hydrogen on oil-induced pre-ignition

The lubricant base oil consists of large hydrocarbon (HC) molecules, which may undergo auto-ignition if oil droplets from the top-land crevice or other sources evaporate during the engine compression stroke. This pre-ignition mechanism consists of three stages – oil droplet introduction into the combustion chamber, evaporation and auto-ignition. This section focusses on the later – we used a diesel injector to inject and atomize a small quantity of n-heptane (~8-20 mg/injection) as a surrogate for a high cetane number base-oil hydrocarbon and observed the H_2 effect on the ignition. The HC ignition is highly sensitive to mixing history, which can be modified by changing the fuel injection duration and pressure. Three injection pressure/duration combinations were tested with the resulting in-cylinder pressure traces presented in Figure 7. Case 1 (Figure 7a) presents a large injection case (20 mg/inj.), with higher injection pressure and duration. The ensemble-averaged pressure traces show an unexpected but significant clear trend of increasing ignition delay and cyclic variability with increasing ϕ_{H2}. This result suggests that H_2 inhibits autoignition reactions of hydrocarbons, delays the pre-ignition, and likely reduces the probability of pre-ignition. This trend also applied to smaller (8 mg/inj.) injections in Figure 7b-c. The inhibition effect in these cases was even stronger, with many cycles failing to ignite as ϕ_{H2} exceeded 0.2-0.3.

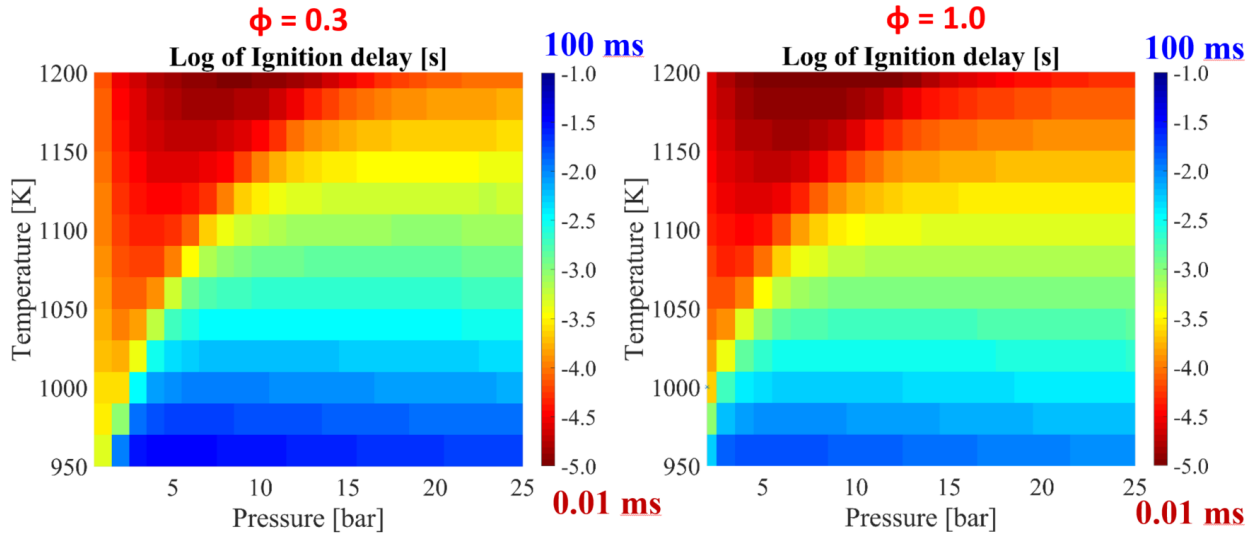

Figure 6: H2-air mixture constant-pressure homogeneous reactor ignition delay sensitivity (false-color scale) to pressure and temperature at ultra-lean (ϕ = 0.3, left) and stoichiometric conditions (right).

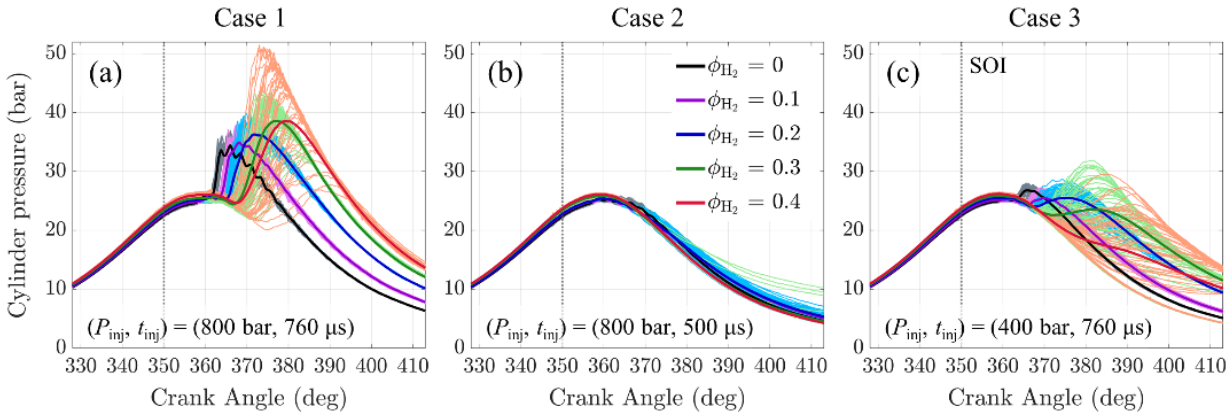

Figure 7: In-cylinder pressure trace dependence on premixed H_2 equivalence ratio (ϕ_{H2}) for three n-heptane injection strategies (a-c) distinguished by injection pressure and duration. Bold traces are ensemble-averages, with thin traces representing individual cycles.

Chemical kinetics simulations using a homogeneous reactor with a detailed H_2 kinetics mechanism were employed to gain further insight into the impact of ϕ_{H2} on autoignition of hydrocarbons and explain the increased delay/sensitivity of shorter injections. The reactor was initialized with mixtures of varying equivalence ratios of n-heptane and air ($\phi_{heptane}$) for various values of ϕ_{H2}. As shown in Figure 8(right), the cool-flame (dashed) and high-temperature (full line) ignition delays (ID) for H_2/heptane blends were extracted from the calculated temperature trace. These results show that increasing the ϕ_{H2} strongly increases the heptane ID at lean $\phi_{heptane}$, which results in strong shift of the most reactive mixture fraction towards fuel-rich conditions. This explains the strong increase in ID of short pilot-fuel injections tested in this work. However, in fuel-rich $\phi_{heptane}$, the impact of H_2 is weaker and the ID increases only moderately. This indicates that larger slow-evaporating oil droplets emitted from the top-land crevice that form fuel-rich mixtures near the droplet surface could be more significant sources of pre-ignition than atomized and well-mixed oil droplets. Additionally, following combustion, the oil droplets might coke and form hot glowing particles that can remain in the combustion chamber even after the exhaust stroke and potentially resulting in pre-ignition [19]. These findings set the future research direction to investigate the evaporation and combustion characteristics of single oil droplets injected at low velocity into compressed or burnt H_2-air charge.

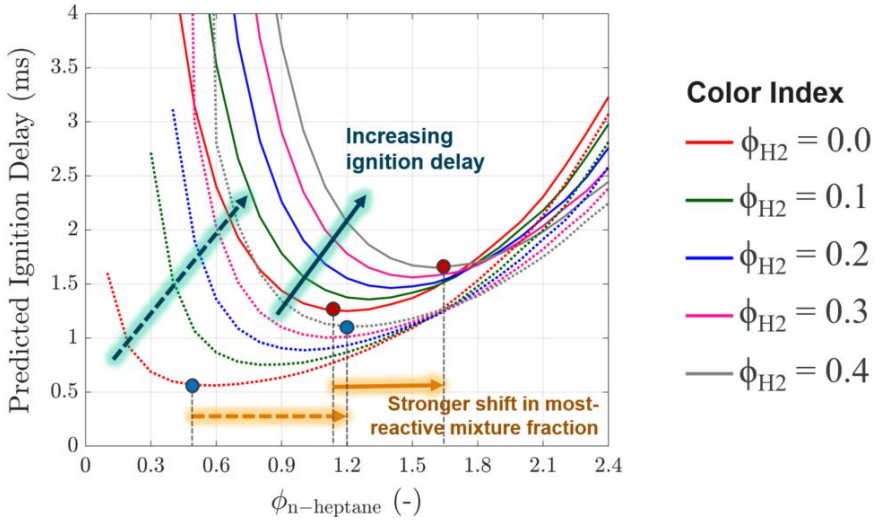

Figure 8: Homogeneous-reactor calculated cool-flame ignition delay (dotted line) and high-temperature ignition delay (full line) dependence on the equivalence ratio of hydrocarbon fuel ($\phi_{n\text{-heptane}}$) and premixed fuel (ϕ_{H2}) in air at 797 K and 23 bar.

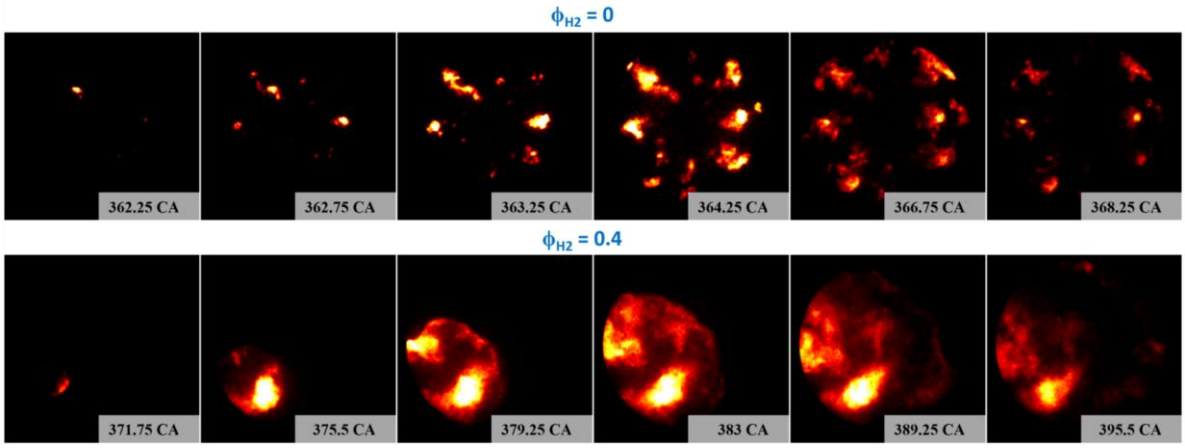

Figure 9: Representative cycle OH* chemiluminescence high-speed image sequence for 800 bar 760 µs fuel injection at (a) ϕ_{H2} = 0 and (b) ϕ_{H2} = 0.4

The impact of H_2 on the combustion evolution for a large pilot-injection is visualized by flame luminosity image sequences in Figure 9. All eight injector sprays ignite and form individual flame kernels within 1°CA after first flame luminosity is detected at 362.25 CA, characteristic of stable and repeatable combustion of the n-heptane fuel jets. Under otherwise unchanged conditions at ϕ_{H2} = 0.4, ignition is delayed by ~9°CA and flame propagates from a single ignition kernel in a manner similar to a spark ignition combustion process. The intensity variations in flame luminosity long after ignition (after ~380 CA) are caused by variations in local equivalence ratio (ϕ_{H2} + $\phi_{n\text{-heptane}}$) rather than through formation of new autoignition kernels. This is in agreement with the homogeneous reactor results (Figure 8) which shows strong ignition inhibition in fuel lean n-heptane-air mixtures. The chemiluminescence evolution suggests that ignition initiated from a single location with a higher local equivalence ratio of HC fuel. Analogously, a slowly-moving oil droplet which creates high local equivalence ratio is likely going to be significantly less impacted by H_2 than well-dispersed HC vapors from wall lubricant vaporization or similar sources. Future testing will explore this impact along with investigations into the role of oil composition as discussed below.

3.3 The role of combustion residuals

Hot combustion residuals that are not scavenged during the exhaust stoke remain within the combustion chamber at the start of the intake stroke and may reside within valve and piston crevices, the spark-plug insulator crevice volume, and inside a pre-chamber igniter for a prolonged period even after the combustion chamber residuals were fully mixed with the fresh intake charge. Auto-ignition reactions may trigger pre-ignition and/or back-fire at the interface between the fresh charge and the combustion residuals [18]. The optical engine configuration has many crevices that may be responsible for residual-induced pre-ignition: pre-chamber, large top-land crevice (42 mm deep, 0.5 mm thick), and crevice within the Kistler 741 pressure sensor switching adapter.

The results shown in this study constitute preliminary results as processing of experimental results is still ongoing. The results suggest a significant sensitivity of pre-ignition to both the temperature of combustion residuals (spark timing) and residual residence time after intake valve opening (pressure difference between the intake and exhaust manifold at IVO). At positive scavenging pressure (intake pressure higher than exhaust), the efforts to induce pre-ignition by continuously delaying the spark timing at H_2 equivalence ratio of up to ϕ = 0.4 and 1 bar intake pressure proved challenging. Spark timings as late as 80°CA after TDC produced no pre-ignition or back-fire. Figure 10a shows pressure traces for a fired cycle and the succeeding cycle intake and compression stroke. The spark is triggered about 45°CA before the exhaust valve opening (EVO) and produces noticeable pressure rise in the pre-chamber. Pressure in the main chamber begins to rise soon after and continues to rise even after the EVO, indicating that the combustion is not complete by the EVO. Therefore, the combustion residuals may be as hot as the adiabatic flame temperature at ϕ=0.4, about 1400°K. Yet, none of the cycles experienced pre-ignition despite the high residual temperature.

Homogeneous reactor simulations suggest H_2 ignition delay might be as short as 100 µs when fresh mixture adiabatically mixes with combustion residuals at 1400 K. Due to the pressure difference between the intake and exhaust manifolds of about 0.4 bar, the fresh mixture rushes into the cylinder and mixes with the residuals, thus reduces the contact time when hot residuals are mixing with fresh mixture and mitigates the pre-ignition.

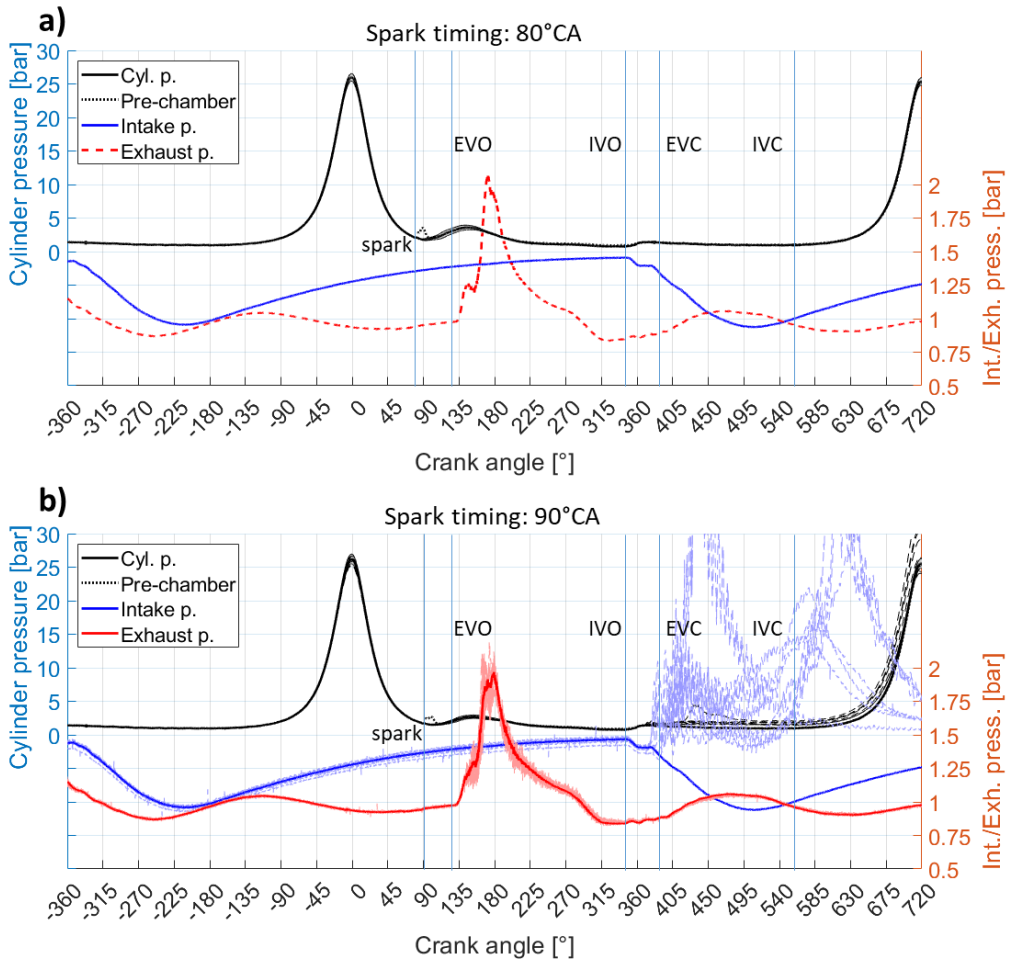

Figure 10: Cylinder pressure, pre-chamber pressure, intake and exhaust pressure traces for spark timing at (a) 80°CA aTDC and (b) 90°CA aTDC. Ensemble-averaged traces are shown with solid lines with 2σ cyclic variability shown as lighter shade. Pre-igniting cycles are shown with dashed line on (b).

About 20% of cycles begun backfiring when the spark was delayed by an additional 10° to 90°CA after TDC. This delay did not change the phenomenology or repeatability of combustion before EVO as visible by comparing Figure 10 a) and b) – the temperature of combustion residuals was not significantly influenced. Optical imaging was used to understand the differences between the normal and back-firing cycles at this operating conditions.

Figure 11 shows high-speed IR imaging around the time of IVO at 347°CA – IR emission from hot cylinder head components as well as the IR emission from hot water vapor are visible. A normal cycle (Figure 11 top) shows rather slow-moving pockets of hot water vapor until 347°CA – at this timing, the inrush of fresh mixture (intake valves are at the top of the image) rapidly mixes with combustion residuals and diminishes the IR emission. The back-firing cycle (Figure 11b) shows brighter IR emission before IVO, stratified to bottom-left region of engine combustion chamber. At IVO, the IR emission becomes dimmer but is not fully eliminated. This indicates that combustion residuals poorly mixed with the fresh charge or that combustion from previous cycle was still ongoing at IVO, which readily ignited the fresh charge.

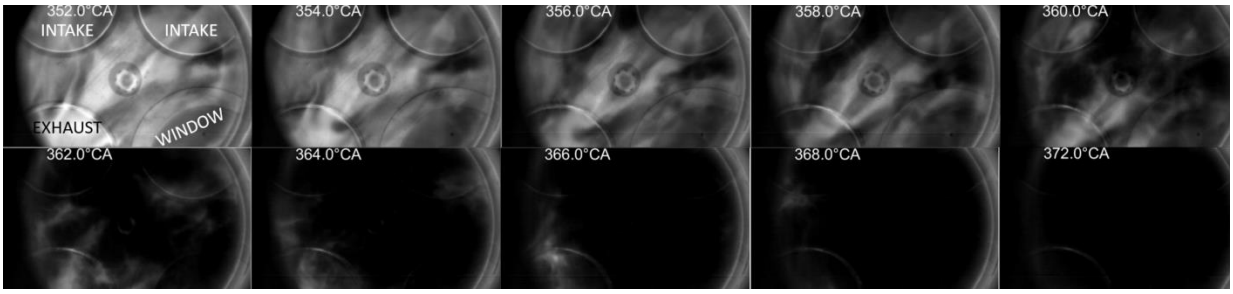

(a) Normal cycle

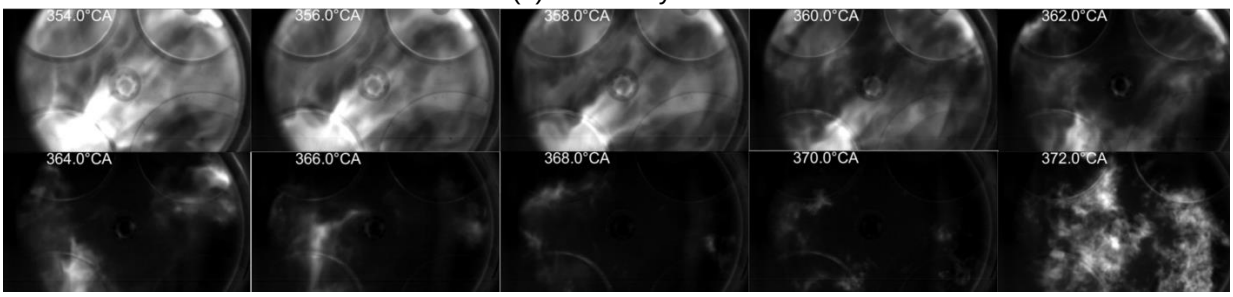

(b) Pre-igniting cycle

Figure 11: IR image series for spark timing at 90°CA aTDC for (a) representative normal cycle and (b) representative back-firing cycle.

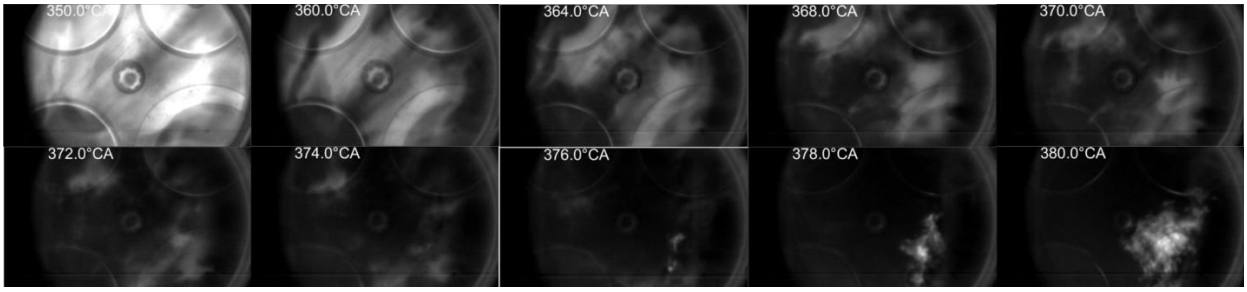

Figure 12: IR image serials for a pre-igniting cycle at spark timing of 45° aTDC under conditions with matching intake and exhaust pressure at IVO.

The high-speed OH* imaging (not shown here) provided insight into the main reason for back-fire of cycle in Figure 111b. The OH* emission recorded simultaneously with IR images around the IVO timing indicates that pockets of unburnt mixture from previous cycle remained until the time of IVO as indicated by presence of OH* emission. While the inrush of fresh mixture extinguished some of the remaining flame pockets, OH* emission re-emerged soon after the IVO. This phenomenology of back-fire was consistent in all recorded cycles.

The investigations at a reduced pressure difference between the intake and the exhaust manifold at IVO suggest that back-fire and pre-ignition are possible even at significantly earlier spark timing, with reduced temperature of combustion residuals, also in cycles where OH* imaging does not suggest any reacting pockets remaining until the IVO. Figure 12 shows a series of IR images showing a backfire event that was not caused by late combustion from previous cycle as seen on Figure 11. Because of the lower pressure difference between the intake and exhaust manifolds at IVO, the residual scavenging is much slower – images at both 350°CA and 360°CA show widespread presence of combustion residuals, compared to cycles shown in Figure 11 where residuals are mostly scavenged and mixed by latest 364°CA. A pocket of hot residuals is visibly lingering in the bottom-right section of the image for a prolonged time, surrounded by fresh mixture indicated by lower IR intensity in the surrounding regions. This pocket of residuals is responsible for triggering local auto-ignition at 376°CA (16°CA into the subsequent cycle), with a growing flame kernel indicated by bright IR imaging visible in the subsequent images.

The data presented here is only a subset of a comprehensive dataset with a range of tested fuel equivalence ratios, and finely tuned pressure difference between the intake and exhaust

pressure, thus covering a range of residual temperatures and residence times. Analysis is currently underway to develop 0D/1D models that will be able to predict the pre-ignition cycles based on the estimated residence time and residual temperature in operating H2 engines. Additionally, the database generated in this study can serve to validate 3D-CFD models of pre-ignition when used to study pre-ignition occurring due to hot residuals in crevices or inside pre-chambers.

4 SUMMARY AND CONCLUSIONS

This manuscript summarizes the past efforts of Combustion Research Facility at Sandia National Laboratories to develop a conceptual understanding of pre-ignition processes in heavy-duty H2ICE by using the concept of artificially induced pre-ignition. This concept allows us to individually characterize different mechanisms of pre-ignition by introducing controlled artificial sources of pre-ignition decoupled from engine load and operating conditions while utilizing the engine optical accessibility to provide further insight into the relevant mechanisms. Four pre-ignition sources have been explored so far – hot-spot, catalytic effects, combustion residuals, and some aspects of oil-induced pre-ignition.

The experimental and modelling results support the following conclusions and further research needs:

Hot-spot pre-ignition:

Surface temperature exceeding 1100 K was required to trigger pre-ignition of H_2 when injecting fuel during the intake stroke, with even higher temperature needed for injections during the compression stroke. These temperatures are higher than the hottest surfaces typically present in engine combustion chambers.

The hot-spot pre-ignition timing was clustered during the intake and early compression stroke, with significantly reduced probability for pre-ignition to occur during late compression stroke when in-cylinder pressure and temperature were high. Chemical kinetics simulations suggest that elevated pressure freezes the auto-ignition reactions of H_2, which explains the above observation. Therefore, hot-spot pre-ignition can be effectively mitigated by delaying the injection timing until sufficiently high in-cylinder pressure is reached during the compression stroke.

Platinum catalytic effects were shown to have a minor effect on pre-ignition probability or temperature threshold for hot-spot pre-ignition. Use of catalytically active metals in spark plug electrodes appears unlikely to worsen the pre-ignition.

The hot-spot in current tests was fairly exposed to in-cylinder flows which shortened the residence time of fuel in the hot regions. Future testing with shielded hot-spot with longer residence time is needed to obtain a full image.

Oil-induced pre-ignition:

The preliminary testing revealed that H_2 significantly inhibits auto-ignition reactions of fuel-lean well-mixed hydrocarbon mixtures. The effect is less pronounced as the hydrocarbon equivalence ratio increases. These results suggest that H_2 engines might be less prone to oil-induced pre-ignition than comparable natural gas or liquid fueled engines.

The evaporation of oil droplets in the engine combustion chamber likely induces long-persisting regions with high hydrocarbon equivalence ratio near the droplet surface in contrast to fast evaporation and mixing experienced by pilot-fuel jets injected into H_2/air mixture.

Future testing will explore the impact of oil-droplet size and injection timing on the tendency to induce pre-ignition. The proposed experimental methodology will also allow us to explore the effects of oil composition and potential coking on pre-ignition tendency.

Combustion-residual role in pre-ignition:

The tested configuration featured combustion residuals trapped inside the pre-chamber and pressure sensor switching adapter cavity in addition to main-chamber residuals. The temperature of combustion residuals was controlled by delaying the spark timing while motoring the engine, using fuel fumigation as the most pre-ignition prone fuel injection approach. Additionally, the combustion residual residence time was varied by adjusting the pressure difference between the intake and exhaust manifolds.

At positive scavenging pressure, we were unable to induce pre-ignition by combustion residuals even with residuals temperature as high as 1400 K unless the in-cylinder combustion was still on-going at the time of intake valve opening due to excessively delayed spark timing.

However, investigations at equal intake and exhaust pressure at IVO showed a significantly increased pre-ignition propensity, which was attributed to prolonged residual residence time due

to the slower inrush of fresh mixture at IVO. Data analysis is underway to develop calibrated 0D/1D models for predicting pre-ignition while the generated database can serve for validation of more complex 3D CFD efforts.

5 ACKNOWLEDGEMENTS

Optical engine experiments were conducted at the Combustion Research Facility of Sandia National Laboratories in Livermore, CA. We gratefully acknowledge the contribution of Kyra N. Schmidt for her assistance in developing research tools and maintaining the optical engine.

FUTURE WORK

The investigations performed to date combined with understanding from the literature suggest that hot-spot and combustion-residuals are unlikely to be the main contributors to pre-ignition and back-fire [26]. The future investigations need to address the open aspect of hot-spot shielded from strong in-cylinder flow and the aspect of residual preignition at higher equivalence ratio. However, the main focus will shift towards oil droplet and particle induced pre-ignition.

The present results suggest that H_2 inhibits auto-ignition of vaporized and mixed hydrocarbons like those found in lubricant base oil, compared to other fuels like natural gas or gasoline that are less prone to pre-ignition compared to H_2. The results also suggest that this inhibition is weaker under conditions with high concentration of hydrocarbons resulting in fuel-rich mixture. In engines, the oil that enters the engine combustion chamber is not atomized and evaporates rather slowly, creating a pocket of fuel-rich mixture surrounding the droplet. In our future testing we intend to introduce oil droplets into the engine combustion chamber under controlled conditions using the Engine Combustion Network single-hole GDI injector operated at very low injection pressure (~1 bar) and using a short energizing time. Benchtop experiments (Figure 13) demonstrated that this injection strategy produces slow-moving droplets in the 20-100 µm diameter range [27], which covers the expected size range of oil droplets emitted from the top-land crevice. These investigations will allow us to test the importance of droplet size, oil composition, injection timing as well as possible oil coking and particle production. The oil droplet size range smaller than 20 µm will be considered if the results from the initial testing indicate it could be important.

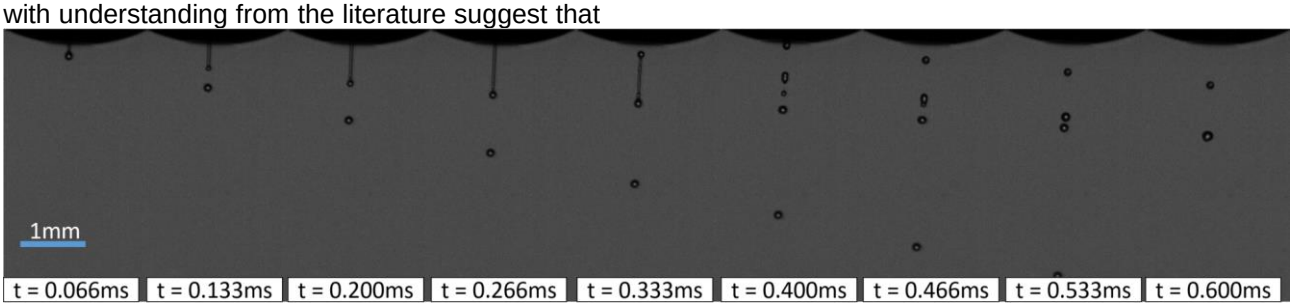

Figure 13: A high-speed diffuse back illumination imaging of droplets emitted from the Engine Combustion Network single hole atomizer at low pressure differential across injector when using short energizing time.

6 REFERENCES

1. Conway, G., Joshi, A., Leach, F., García, A., and Senecal, P.K. 2021. A review of current and future powertrain technologies and trends in 2020, *Transportation Engineering,* 5: p. 100080.
2. Dong, C., Zhou, Q., Zhang, X., Zhao, Q., Xu, T., and Hui, S.e. 2010. Experimental study on the laminar flame speed of hydrogen/natural gas/air mixtures, *Frontiers of Chemical Engineering in China,* 4(4): p. 417-422.
3. Huang, Z., Zhang, Y., Zeng, K., Liu, B., Wang, Q., and Jiang, D. 2006. Measurements of laminar burning velocities for natural gas–hydrogen–air mixtures, *Combustion and Flame,* 146(1): p. 302-311.

4. Chapman, A., Itaoka, K., Hirose, K., Davidson, F.T., Nagasawa, K., Lloyd, A.C., Webber, M.E., Kurban, Z., Managi, S., Tamaki, T., Lewis, M.C., Hebner, R.E., and Fujii, Y. 2019. A review of four case studies assessing the potential for hydrogen penetration of the future energy system, *International Journal of Hydrogen Energy,* 44(13): p. 6371-6382.
5. Nikolaidis, P. and Poullikkas, A. 2017. A comparative overview of hydrogen production processes, *Renewable and Sustainable Energy Reviews,* 67: p. 597-611.
6. Yip, H.L., Srna, A., Yuen, A.C.Y., Kook, S., Taylor, R.A., Yeoh, G.H., Medwell, P.R., and Chan, Q.N. 2019. A Review of Hydrogen Direct Injection for Internal Combustion Engines: Towards Carbon-Free Combustion, *Applied Sciences,* 9(22): p. 4842.
7. Pan, J., Yi, D., Wang, L., Liang, W., Shu, G., and Wei, H. 2023. Understanding multi-regime detonation development for hydrogen and syngas fuels, *Physics of Fluids,* 35(3).
8. Pan, J., Wang, L., Liang, W., Law, C.K., Wei, H., and Shu, G. 2022. Multi-regime reaction front and detonation initiation by temperature inhomogeneity, *Proceedings of the Combustion Institute,* 39(4): p. 4929-4937.
9. Xu, H., Ni, X., Su, X., Xiao, B., Luo, Y., Zhang, F., Weng, C., and Yao, C. 2021. Experimental and numerical investigation on effects of pre-ignition positions on knock intensity of hydrogen fuel, *International Journal of Hydrogen Energy,* 46(52): p. 26631-26645.
10. Meng, H., Ji, C., Yang, J., Chang, K., Xin, G., and Wang, S. 2022. A knock study of hydrogen-fueled Wankel rotary engine, *Fuel,* 321: p. 124121.
11. Dhyani, V. and Subramanian, K.A. 2021. Development of online control system for elimination of backfire in a hydrogen fuelled spark ignition engine, *International Journal of Hydrogen Energy,* 46(27): p. 14757-14763.
12. Kondo, T., Iio, S., and Hiruma, M. 1997. A Study on the Mechanism of Backfire in External Mixture Formation Hydrogen Engines -About Backfire Occurred by Cause of the Spark Plug, *SAE Technical Paper, 971704*.
13. Bates, L., Bradley, D., Paczko, G., and Peters, N. 2016. Engine hot spots: Modes of auto-ignition and reaction propagation, *Combustion and Flame,* 166: p. 80-85.
14. Huyskens, P., Van Oost, S., Goemaere, P.J., Bertels, K., and Pecqueur, M. 2011. The technical implementation of a retrofit hydrogen PFI system on a passenger car, *SAE Technical Paper, 2011-01-2004*.
15. Shinde, B.J. and K, K. 2022. Recent progress in hydrogen fuelled internal combustion engine (H2ICE) – A comprehensive outlook, *Materials Today: Proceedings,* 51: p. 1568-1579.
16. Rönn, K., Swarts, A., Kalaskar, V., Alger, T., Tripathi, R., Keskiväli, J., Kaario, O., Santasalo-Aarnio, A., Reitz, R., and Larmi, M. 2023. Low-speed pre-ignition and super-knock in boosted spark-ignition engines: A review, *Progress in Energy and Combustion Science,* 95: p. 101064.
17. Pan, J., Zheng, Z., Wei, H., Pan, M., Shu, G., and Liang, X. 2021. An experimental investigation on pre-ignition phenomena: Emphasis on the role of turbulence, *Proceedings of the Combustion Institute,* 38(4): p. 5801-5810.
18. Eicheldinger, S., Karmann, S., Prager, M., and Wachtmeister, G. 2022. Optical screening investigations of backfire in a large bore medium speed hydrogen engine, *International Journal of Engine Research,* 23(5): p. 893-906.
19. Shu, G., Dong, L., and Liang, X. 2012. A review of experimental studies on deposits in the combustion chambers of internal combustion engines, *International Journal of Engine Research,* 13(4): p. 357-369.
20. Koyanagi, K., Hiruma, M., and Furuhama, S. 1994. Study on Mechanism of Backfire in Hydrogen Engines, *SAE Technical Paper, 942035*.
21. Gao, J., Wang, X., Song, P., Tian, G., and Ma, C. 2022. Review of the backfire occurrences and control strategies for port hydrogen injection internal combustion engines, *Fuel,* 307: p. 121553.
22. Rajasegar, R., Srna, A., Barbery, I., and Novella, R. 2023. On the Phenomenology of Hot-Spot Induced Pre-Ignition in a Direct-Injection Hydrogen-Fueled, Heavy-Duty, Optical-Engine, *SAE International Journal of Advances and Current Practices in Mobility,* 6(3): p. 1535-1547.
23. Rajasegar, R., Srna, A., and Lee, T. 2023. Impact of Hydrogen on the Ignition and Combustion Behavior Diesel Sprays in a Dual Fuel, Diesel-Piloted, Premixed Hydrogen Engine, *SAE International Journal of Advances and Current Practices in Mobility,* 6(4): p. 1762-1776.
24. Niki, Y., Rajasegar, R., Li, Z., Musculus, M.P., Garcia Oliver, J.M., and Takasaki, K. 2022. Verification of diesel spray ignition

phenomenon in dual-fuel diesel-piloted premixed natural gas engine*, International Journal of Engine Research,* 23(2): p. 180-197.
25. Ó Conaire, M., Curran, H.J., Simmie, J.M., Pitz, W.J., and Westbrook, C.K. 2004. A comprehensive modeling study of hydrogen oxidation*, International Journal of Chemical Kinetics,* 36(11): p. 603-622.
26. D. Takahashi, N.M., A. Yamashita, K. Nakata,, *Toyota's Hydrogen-Engine Development to Contribute to Carbon Neutrality*, in Proceedings of *Vienna Motor Symposium*. 2023.
27. Bhoite, S., Windom, B., Singh, J., Montgomery, D., and Marchese, A.J. 2023. A study of ignition and combustion of liquid hydrocarbon droplets in premixed fuel/air mixtures in a rapid compression machine*, Proceedings of the Combustion Institute,* 39(2): p. 2533-2542.